# Tracking $Ca^{2+}$ Dynamics in NOD Mouse Islets During Spontaneous Diabetes Development

Sandra Postić,[1] Johannes Pfabe,[1] Srdjan Sarikas,[1] Barbara Ehall,[2] Thomas Pieber,[2] Dean Korošak,[3] Marjan Slak Rupnik,[1,3,4] and Ya-Chi Huang[1]

*Diabetes 2023;72:1251–1261 | https://doi.org/10.2337/db22-0952*

**The mechanisms accounting for the functional changes of α- and β-cells over the course of type 1 diabetes (T1D) development are largely unknown. Permitted by our established technology of high spatiotemporal resolution imaging of cytosolic $Ca^{2+}$ ($[Ca^{2+}]_c$) dynamics on fresh pancreas tissue slices, we tracked the $[Ca^{2+}]_c$ dynamic changes, as the assessment of function, in islet α- and β-cells of female nonobese diabetic (NOD) mice during the development of spontaneous diabetes. We showed that, during the phases of islet inflammation, 8 mmol/L glucose-induced synchronized short $[Ca^{2+}]_c$ events in β-cells were diminished, whereas long $[Ca^{2+}]_c$ events were gradually more triggerable at substimulatory 4 and 6 mmol/L glucose. In the islet destruction phase, the synchronized short $[Ca^{2+}]_c$ events in a subset of β-cells resumed at high glucose condition, while the long $[Ca^{2+}]_c$ events were significantly elevated already at substimulatory glucose concentrations. In the α-cells, the glucose sensitivity of the $[Ca^{2+}]_c$ events persisted throughout the course of T1D development. At the late islet destruction phase, the α-cell $[Ca^{2+}]_c$ events exhibited patterns of synchronicity. Our work has uncovered windows of functional recovery in β-cells and potential α-cells functional synchronization in NOD mice over the course of T1D development.**

## ARTICLE HIGHLIGHTS

- In NOD mice β-cells, 8 mmol/L glucose–induced synchronized short $[Ca^{2+}]_c$ events diminish in the early phases of islet inflammation, and long $Ca^{2+}$ events became more sensitive to substimulatory 4 and 6 mmol/L glucose.
- In the late islet destruction phase, the synchronized short $[Ca^{2+}]_c$ events in a subset of β-cells resumed at 8 mmol/L glucose, while the long $Ca^{2+}$ events were significantly elevated at substimulatory glucose concentrations.
- In the α-cells, the glucose sensitivity of the $[Ca^{2+}]_c$ events persisted throughout the course of type 1 diabetes development.
- α-Cell $[Ca^{2+}]_c$ events occasionally synchronize in the islets with severe β-cell destruction.

Type 1 diabetes (T1D) is characterized by selective autoimmune destruction of the insulin-secreting β-cells and dysregulation of the glucagon-secreting α-cells within the islets of Langerhans (1,2). To date, the mechanisms accounting for the pathophysiology of β- and α-cells during the development of T1D disease remain largely unknown. This is, in part, due to a lack of means to adequately preserve the inflamed and structurally damaged islets in the T1D pancreas. The conventional methods of islet isolation inevitably impose enzymatic and mechanical disturbances to T1D islets, resulting in systemically biased experimental outcome that is not exclusive to T1D pathogenesis per se (3). Moreover, owing to the spontaneous onset of T1D, it is not possible to determine the phases of disease progression by judging solely from the animal in vivo parameters. Frequently, when overt hyperglycemia manifests at the onset of the disease within subjects with T1D, their islets have already undergone severe immunogenic assault, and up

[1]Center for Physiology and Pharmacology, Medical University of Vienna, Vienna, Austria
[2]Division of Endocrinology and Diabetology, Department of Internal Medicine, Medical University of Graz, Graz, Austria
[3]Faculty of Civil Engineering, Transportation Engineering and Architecture, University of Maribor, Maribor, Slovenia
[4]Alma Mater Europaea – European Center Maribor, Maribor, Slovenia

Corresponding authors: Marjan Slak Rupnik, marjan.slakrupnik@meduniwien.ac.at, and Ya-Chi Huang, ya-chi.huang.chum@ssss.gouv.qc.ca

Received 15 November 2022 and accepted 25 May 2023

This article contains supplementary material online at https://doi.org/10.2337/figshare.23223260.

to 80% of β-cells have been depleted (4,5). As a result, there is a marked gap between the onset of autoimmunity and the onset of T1D disease, wherein the pathophysiological changes of the α- and β-cells, to a large extent, are not yet described. Thereby, the development of therapeutic interventions targeting β-cell rescue and α-cell function restoration are currently limited. Accordingly, a thorough investigation following the islet cells functional changes within this gap would offer valuable opportunities for early diagnosis and prevention of the diseases.

For two decades, we have invested much effort in developing the pancreas tissue slices preparation that successfully circumvented one of the longstanding challenges in properly preserving T1D islets and the intraislet cell-cell interactions for pathophysiology investigations. This specific preparation procures islets within thin pancreas tissue slices, is devoid of enzymatic and mechanical stresses inherent in conventional islet isolation, and preserves islet cells within the native cellular milieu of both normal and autoimmune disrupted islets. Our development of the pancreas slice preparation offered unprecedented opportunity, initially, to investigate T1D mouse islet cells via electrophysiological means (3,6,7). Recently, we further extended the application of this preparation to confocal scanning high spatiotemporal resolution microscopy, enabling long-duration tracking of $[Ca^{2+}]_c$ dynamic changes in cells within pancreas slices (8–11).

In this study, we investigated the pathophysiology of T1D islets by tracking the islet α- and β-cell $[Ca^{2+}]_c$ dynamics (up to several hundred cells) within female NOD mice at an age window relevant to disease development. This approach overcame the major research difficulties stemming from the spontaneous onset of diabetes in NOD mice. Here, we provide insights into the functional changes of islet α- and β-cells in parallel with changes in both the islet morphology and the in vivo parameters in NOD mice during the progression of T1D.

## RESEARCH DESIGN AND METHODS

### Animals

All protocols were approved by the Federal Ministry of Education, Science and Research of the Republic of Austria, Vienna, Austria (permit number 2020-0.258.669). Female NOD mice develop spontaneous diabetes as early as 90 days of age (~13 weeks), and, by the age of 30 weeks, the incidence of female NOD mice developing overt diabetes is 80% (12). We thus used 13 female NOD mice (NOD/ShiLtJ; The Jackson Laboratory) aged between 13 and 22 weeks, aimed at capturing the islets' range from no immunogenic disturbances to full-blown islet destruction. The NOD mice were kept on a 12:12 h light:dark schedule in individually ventilated cages or subjected to pancreas slice preparation. Two to six islets from each NOD mouse, prepared in pancreas slices, were subjected to live-cell imaging of $[Ca^{2+}]_c$ dynamics. This is based on the notion that sampling two to six islets per mouse in the 13 NOD female mice would result in a sample size of at least five islets in each of the seven phases of T1D islet autoimmune destruction (described below). The pancreas slice preparation procedures were described previously (6,7,13) and in the Supplementary Material.

### Blood Glucose and Serum Insulin Measurements

Each NOD mouse was euthanized by $CO_2$ overdose, followed by cervical dislocation. Blood glucose was measured from the tail vein (glucometer; Ascensia), and serum insulin level was measured (Insulin Ultra-Sensitive assay kits; Cisbio, Codolet, France) from whole blood collected by cardiac puncture.

### Dynamic $[Ca^{2+}]_c$ Imaging

Dynamic $[Ca^{2+}]_c$ imaging was performed on a Leica TCS SP8 inverted confocal system (20×, NA 1.0). Each tissue slice was transferred into an imaging chamber that was continuously perfused with warm (34°C) HEPES-buffered extracellular solution supplemented with various glucose concentrations. The acquisition frequency was 20 Hz at 256 × 256 pixels resolution and approximately 1-$\mu m^2$ pixel size. Calbryte 520 AM was excited by a 490-nm line of white laser, and emitted light was detected by a Leica HyD hybrid detector in the range of 500–700 nm, using a photon counting mode (Leica Microsystems, Wetzlar, Germany). Each islet $[Ca^{2+}]_c$ dynamic recording lasted ~4,500 s (~75 min), which was designed to complete the perfusion protocol of 4-6-8-6 mmol/L glucose. Exposure to 4 and 6 mmol/L glucose concentrations was 15 min, whereas the 8 mmol/L glucose condition lasted 30 min.

### Analytical Procedure

Analyses of $[Ca^{2+}]_c$ recordings were described previously (14–16). Briefly, the regions of interest (ROIs) were automatically detected using custom Python scripts (Python Software Foundation, Wilmington, DE) (Fig. 1*C* and *D*). Then, information regarding the time profile of $[Ca^{2+}]_c$ changes, the spatial coordinates of the ROIs, neighboring ROIs, movie statistics, recording frequency, and pixel size were sampled. Subsequently, all the significant changes of $[Ca^{2+}]_c$ at all realistic time scales within each ROI were automatically distilled and annotated as events (with $z$ score $> 3$). The events were characterized by the start time and the width at half of their peak amplitude (half-width). According to the different patterns of temporal summation of β-cell $Ca^{2+}$ events in a normal-like islet (Supplementary Fig. 1), we further analyzed the $Ca^{2+}$ events as short (2.5- to 20-s half-width) and long (20- to 200-s half-width) events. α-Cell $Ca^{2+}$ events did not show a noticeable pattern of temporal summation (data not shown); we thus analyzed all α-cell $Ca^{2+}$ events (half-width between 2.5 and 200 s) collectively.

### Network Analysis

We constructed functional networks and computed the mean network degree of each islet from the calcium dynamics in β- or α-cells, using open Python library NetworkX, in

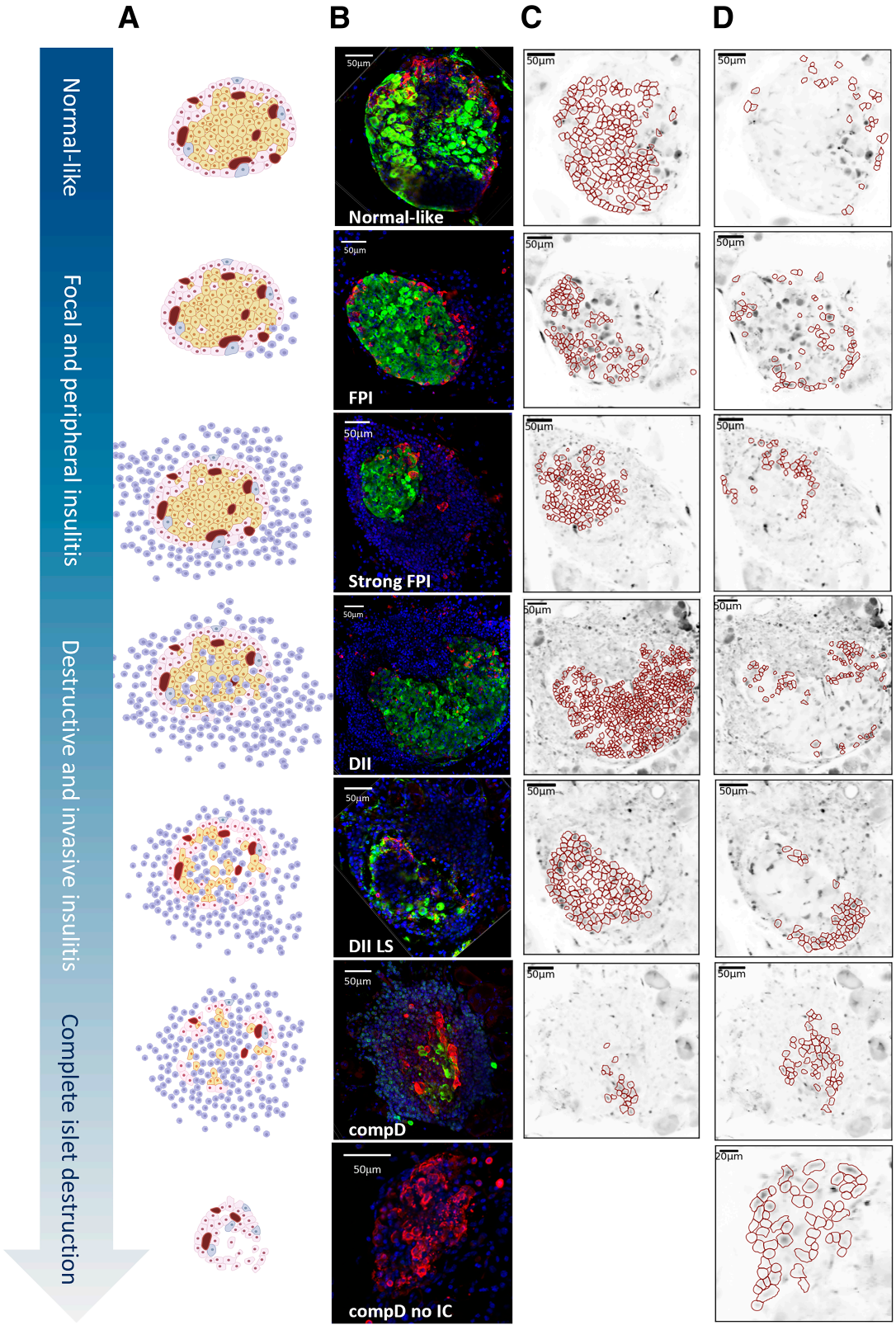


**Figure 1**—Categorization of islets along the severity of T1D diseases. (*A*) Schematic diagram showing islets with progressive severity of immunogenic assault and β-cell destruction. (*B*) Representative islets of each islet group immunoassayed for insulin (green), glucagon (red), and DAPI (blue). Note the normal-like islet shown. This islet has a compact encapsulated structure, insulin- and glucagon-positive cells distributed in accordance with a rodent islet, and no immune cells infiltration observed, and the dynamic $Ca^{2+}$ responses of the β- and α-cells within resembled those in the other islets of the same group; hence, we concluded that the hollows shown in this islet resulted from further processing of the tissue for immunoassays, and have included this islet in the normal-like group. (*C* and *D*) ROIs (in red) representing β-cells (*C*) and in α-cells (*D*).

two steps. First, correlations $c(i,j)$ for all pairs $(i,j)$ of cells are obtained from recorded time series of calcium activity, and then these correlations are compared with the chosen threshold value c0 (0.8 and 0.35 for β- and α-cell collectives, respectively [14]) . If correlation of a cell pair $(i,j)$ exceeds the threshold value, $c(i,j,t) > c0$, the link $(i,j)$ is placed in the network between the nodes representing this cell pair.

### Immunoassays and Antibodies

After $[Ca^{2+}]_c$ imaging, each pancreas slice was collected for immunoassays. Briefly, slices were fixed with 4% paraformaldehyde, permeabilized with 0.3% Triton X, treated with primary rabbit anti-insulin (1:100 dilution, ABclonal) and mouse anti-glucagon (1:200 dilution, Invitrogen) antibodies, and then stained with secondary antibodies (1:500 dilution; goat anti-mouse DyLight 550, and anti-rabbit IgG Alexa 647). To assess the morphology of the islets and the severity of islet immune cell infiltration, we counterstained the slices with DAPI (0.1 μg/mL in PBS).

The pancreas slices were imaged with a confocal microscope (Nikon A1R), excited with 405-, 561-, and 640-nm lasers and detected at 425–475 nm (DAPI), 570–620 nm (DyLight 550), and 663–738 nm (Alexa 647) using GaAsP photomultiplier tube (PMT) detectors. The excitation cross talk was minimized by sequential scanning. Images captured from the slices were used to confirm the localization of α- and β-cells by overlapping the glucagon- and insulin-positive area with the ROIs, created by customed Python scripts, in the $[Ca^{2+}]_c$ recordings. We estimated the overall overlap between the functional and morphological colocalization to be about 80%, taking into account interferences that may occur because of further processing of tissue slices for immunoassays.

### Morphological Classification of the Islets

All islets sampled from the 13 NOD mice were examined blindly by two observers (Y.-C.H. and S.P.) and independently from the mouse of origin, then categorized into groups of increasing severity of islet destruction following a predefined classification adapted from previous studies (5,17): *normal-like*, compact islet architecture and no detectable immune cells in and around the islet; *focal to peripheral insulitis* (FPI), only focal or few immune cells around the islet; *strong FPI*, extensive immune cells infiltrating around the islet, but preserved compact insulin antibody-stained area in the islet; *destructed islets with invasive insulitis* (DII), extensive immune cells surrounding and infiltrating the islet, and less than 50% of β-cell loss as estimated by the insulin-positive area; *DII at late stage* (DII LS), extensive immune cells surrounding and infiltrating the islet, and more than 50% of β-cell loss as estimated by the insulin-positive area in the islet; *near complete destruction of β-cells* (compD), extensive immune cells surrounding and infiltrating the islet, and more than 80% of islet β-cells destruction; and *compD with no remaining immune cells* (compD no IC), more than 80% of islet β-cell destruction, and no more noticeable immune cells surrounding and infiltrating the islet (Fig. 1).

### Distribution of Mice According to Severity of Disease Progression

Based on the average degree of β-cell destruction and immune cell infiltration in islets of each NOD mouse, we distributed the NOD mice into a disease severity spectrum (see Fig. 6*A* for details), representing the pathophysiological progression of spontaneous diabetes from its onset.

### Statistical Analysis

Events detected in the temporal $[Ca^{2+}]_c$ dynamic profiles of every ROI were processed as frequency of $Ca^{2+}$ events (events/min/ROI), which was then averaged across all ROIs of β- or α-cells within an islet and expressed as mean $Ca^{2+}$ events frequency (events/min/ROI ± SEM). Repeated measures two-way ANOVA was conducted to compare the mean $Ca^{2+}$ event frequencies at 4, 6, and 8 mmol/L glucose across all islet groups, followed by post hoc pairwise comparisons using the Tukey multiple comparison test. One-way ANOVA was conducted to compare network connectivity between islet groups, followed by post hoc pairwise comparisons using the Tukey multiple comparison test. Statistical significance is indicated with asterisks, as follows: $*P < 0.05$; $**P < 0.01$; $***P < 0.001$. Statistical analyses were conducted using GraphPad (GraphPad Software, San Diego, CA). All graphics were produced using BioRender software.

### Data and Resource Availability

All data generated or analyzed during this study are included in the published article (and the Supplementary Material). No applicable resources were generated or analyzed during the current study.

## RESULTS

The results present the analyses of $[Ca^{2+}]_c$ dynamic videos of 45 islets from 13 female NOD mice categorized into the seven phases along the pathological progression of T1D islet destruction (Fig. 1 and Supplementary Table 1). Below, the functional changes of islet β- and α-cells (Fig. 2 and Fig. 3, respectively) during the progression of islet destruction in NOD mice are described.

### Diminished Synchronized $[Ca^{2+}]_c$ Events in β-Cells of NOD Mouse Islets at the Onset of Immune Cell Infiltration

β-Cells in the normal-like islet group exhibited the typical $[Ca^{2+}]_c$ dynamic responses in response to 4, 6, and 8 mmol/L glucose (Fig. 2*A*), similar to what we reported in healthy C57/B6J mice (15), suggesting the function of β-cells was not yet disturbed in this islet group. The temporal $[Ca^{2+}]_c$ profile at 8 mmol/L glucose condition comprised an initial nonsynchronized transient phase, frequently superimposed by long $[Ca^{2+}]_c$ spike events (20 to 200 s half-width), followed by a prolonged plateau phase that was superimposed mostly by

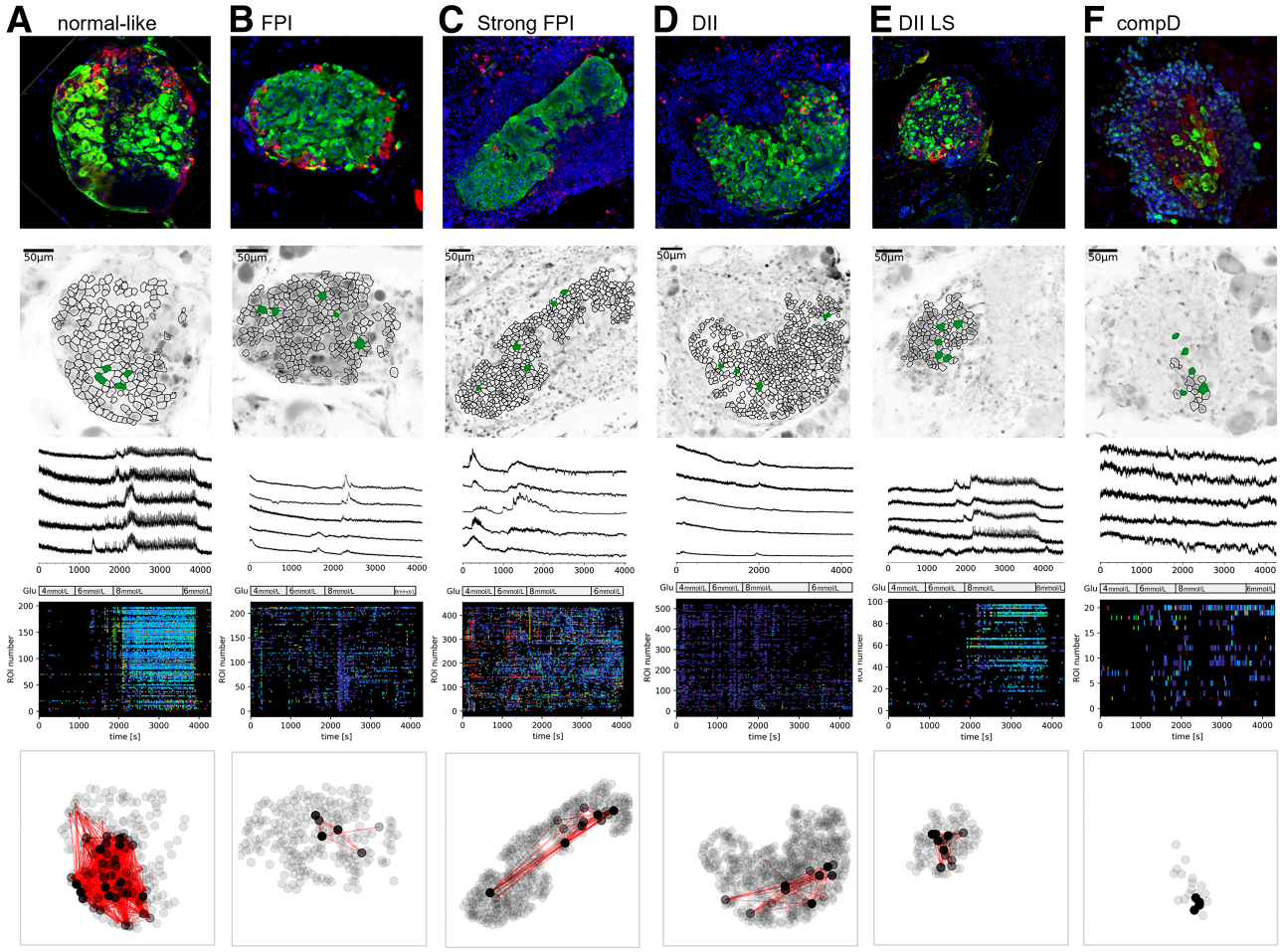


**Figure 2**—$[Ca^{2+}]_c$ dynamics in islet β-cells along autoimmune destruction. Representative islets of normal-like (*A*), FPI (*B*), strong FPI (*C*), DII (*D*), DII LS (*E*), and compD (*F*) groups. The top horizontal panel showed a representative islet of each group, immunoassayed for insulin (green), glucagon (red), DAPI (blue). Second panel showed ROIs of β-cells produced by our segmentation algorithm published previously (16). Note not all insulin-positive areas in the top panel images were taken as ROIs, as some areas were less successfully loaded with the $Ca^{2+}$ indicator. The third row of panels demonstrates five representative $Ca^{2+}$ dynamic profiles extracted from the ROIs that were filled in green. The perfusion protocol is indicated in the bottom bar. The fourth row of panels shows raster plots encoding $[Ca^{2+}]_c$ events detected from all ROIs in temporal sequence. The duration of $Ca^{2+}$ events is color-coded; navy denotes longer and yellow/green denotes shorter events. Only events with a *z* score higher than three are considered statistically significant and included. The traces were rebinned to 2 Hz (recorded at 20 Hz). The bottom row of panels shows the correlation-based functional β-cell network extracted for each islet presented above. Node color intensity reflects the number of functional connections per cell, where black nodes are most connected cells in a 200-s period of the plateau phase after time point 3,000 s during the stimulation in 8 mmol/L glucose.

short $[Ca^{2+}]_c$ events (2.5 to 20 s half-width duration) (Fig. 2*A*), and these events were synchronized across the β-cells in the islet (Fig. 2*A*). The mean frequency of $[Ca^{2+}]_c$ events is summarized in Fig. 4*A* and *B* and Supplementary Table 1. β-Cells in this islet category are highly connected (Fig. 2*A* bottom panel and Fig. 5*A*).

In the islets categorized in the FPI group, representing a T1D pathological phase immediately after immune cells were recruited to the islets, the short $[Ca^{2+}]_c$ events in the plateau phases in β-cells largely disappeared, along with notable decrease in mean degree cellular connectivity (Figs. 2*B* and 4*A* and Supplementary Table 1). The longer $[Ca^{2+}]_c$ events, although glucose dependence persisted, exhibited a tendency of higher responsiveness to 4 and 6 mmol/L substimulatory glucose concentrations (Fig. 4*B*).

As the islet inflammation in the NOD mice aggravates, such as these islets within the strong FPI group, the β-cells showed lowered to complete absence of short $[Ca^{2+}]_c$ events (Figs. 2*C* and 4*A*), with a low number of connections between β-cells (Fig. 5*A*). The long $[Ca^{2+}]_c$ events remained elevated and were no longer glucose dependent (Fig. 4*B* and Supplementary Table 1).

### β-Cells in NOD Mice Exhibited a Short Window of Functional Recovery During the Islet Destruction Phases

Islets in DII and DII LS groups, which resemble the β-cell destruction phases of the NOD islets, showed a transient reappearance of the synchronized short $[Ca^{2+}]_c$ events among the remaining β-cells (Fig. 2*D*–*E*). The β-cell mean

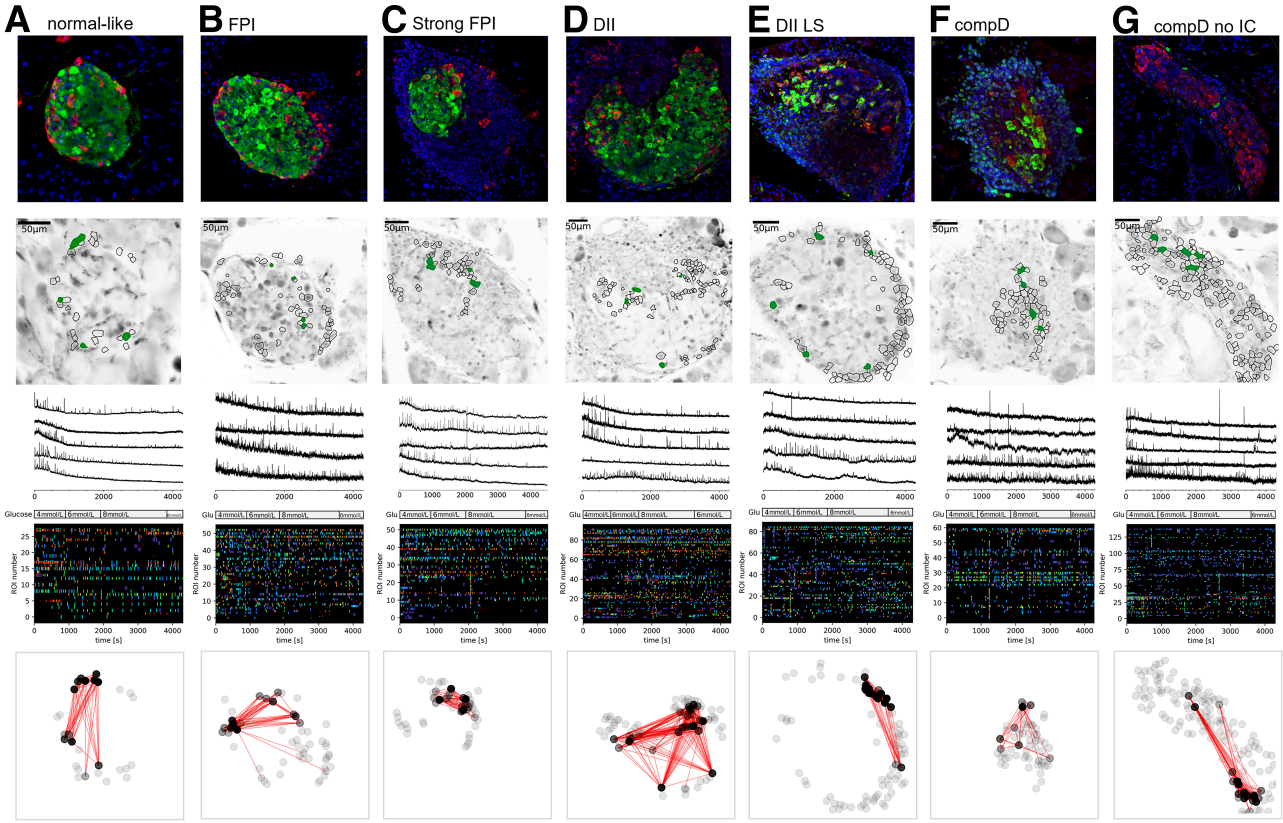


**Figure 3—**$[Ca^{2+}]_c$ dynamics in islet α-cells along autoimmune destruction. The same sequential image display as in Figure 2 was adopted. Note in *E–G*, synchronized $Ca^{2+}$ events, shown as vertical lines at same time points in the raster plots, can be occasionally observed. Some ROIs were determined as α-cells, although not coordinated with a glucagon-positive area on the top panel, because their $Ca^{2+}$ responses were similar to other α-cell ROIs and their orientations were in the islet outer layer. Also, not all glucagon-positive areas were processed into ROIs, because of sometimes less successful loading of the $Ca^{2+}$ indicator in some cells. The black nodes in the bottom panel are the most connected cells in a 200-s period after time point 0 s during the stimulation in 4 mmol/L glucose.

degree connection at the DII LS stage also increased, although it did not reach statistical significance (Fig. 5). The mean frequency of short $[Ca^{2+}]_c$ events significantly increased when glucose concentration was elevated from 6 to 8 mmol/L glucose (Fig. 4*A* and Supplementary Table 1). The long $[Ca^{2+}]_c$ events in the β-cells in DII group were readily triggered at 4 and 6 mmol/L glucose conditions (Fig. 2*D* raster plot, Fig. 4*B*, and Supplementary Table 2).

The recovery of the short $[Ca^{2+}]_c$ events in the β-cells, however, did not persist in the compD islet group (Figs. 2*F* and 4*A* and Supplementary Table 1). Neither did the parameters of network connectivity (Fig. 5*A*).

### Persistent Glucose Sensitivity and Synchronized $[Ca^{2+}]_c$ Events in α-Cells When Spatially Clustered

At 4 mmol/L glucose, α-cells in islets of the normal-like group exhibited a mean $[Ca^{2+}]_c$ event frequency of 0.348 ± 0.111 events/min/ROI, which declined significantly when glucose concentration was raised to 6 mmol/L (0.266 ± 0.133 events/min/ROI; $P$ value $< 0.05$). At 8 mmol/L glucose, the mean frequency further dropped to 0.229 ± 0.129 events/min/ROI (Figs. 3*A* and 4*C*). Remarkably, a repeated measures ANOVA test suggested glucose concentration as a strong source of variance ($P$ value $< 0.0001$) contributing to the $[Ca^{2+}]_c$ responses of α-cells in all islet groups (Fig. 4*C*).

One notable feature within the islets categorized in the DII LS, compD, and compD no IC groups was the occasional synchronized $Ca^{2+}$ events among the α-cells. This observation suggested potential cross talk between α-cells (Fig. 3*E–G*), which may have resulted from the spatial aggregation of α-cells due to islet remodeling that was also evident from the images of immunoassayed islets (Figs. 2, 3, and 6). Indeed, the connectivity among α-cells was significantly increased in the compD no IC group (Fig. 5*B*).

### Islet Immunogenic Assault and Destruction Happened Before Manifestation of Systemic Hyperglycemia in NOD Mice

To this end, the functional analyses of islet α- and β-cells during the progressive islet autoimmune destruction provided mechanistic bases allowing us to estimate the severity of T1D development in the NOD mice used in this study. We distributed the 13 NOD mice in order according to the extent of T1D disease severity, which was based on the

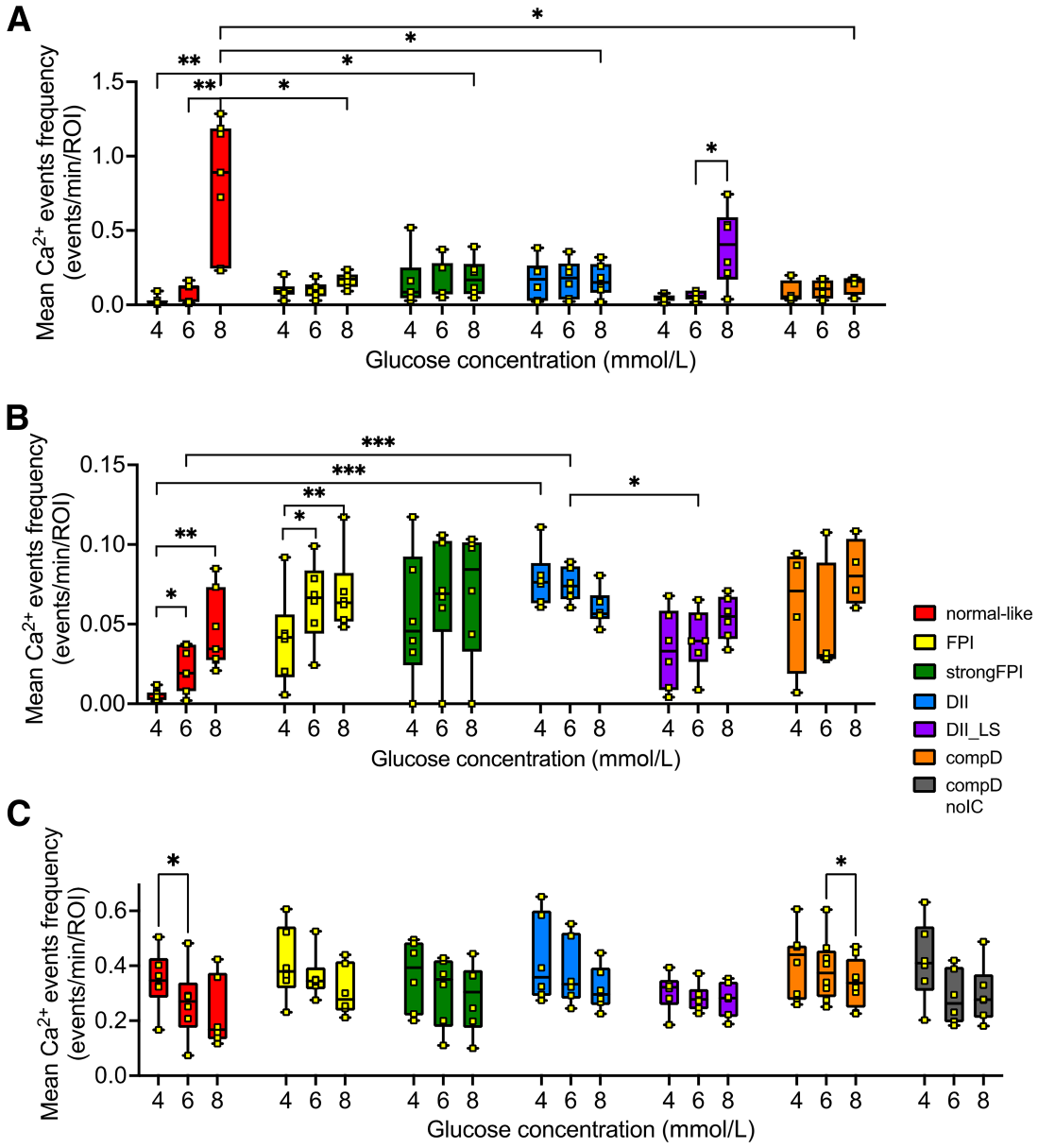


**Figure 4**—Quantification of $[Ca^{2+}]_c$ events in α- and β-cells across all islet groups. (*A*) Short (half-width between 2.5 and 20.0 s) and (*B*) long (half-width between 20.1 and 200.0 s) $[Ca^{2+}]_c$ events of β-cells and (*C*) all $[Ca^{2+}]_c$ events of α-cells (2.5–200.0 s, no segregation of short/long events as no different trends were observed) across all islet groups in response to 4, 6, and 8 mmol/L glucose were quantified into mean frequencies. Note an extra compD no IC group in *C* but not shown in *A*, as no insulin-positive cells were found in islets within this group. Statistical significance is indicated as $*P < 0.05$; $**P < 0.01$; $***P < 0.001$.

islets' overall severity of immune cell infiltration and β-cell destruction and associated with the functional changes in the β- and α-cells of each NOD mouse (Fig. 6*A*). Accordingly, using this distribution of NOD mice we created in Fig. 6*A* and plotted as a function of the age at which each mouse was euthanized, we found no correlation between these two parameters (Fig. 6*B*) ($R^2 = 0.058$), confirming that the onset of T1D is spontaneous and the severity of T1D progression is an asynchronous event (4,5).

Next, we studied the potential association between the distribution of the NOD mice and the serum insulin and plasma blood glucose levels in each NOD mouse (Fig. 6*C*). Hyperglycemia (indicated as 33 mmol/L, the upper limit of the glucometer) (Fig. 6*C* open circles) was detected only in the mice (mice 11–13) bearing islets with profound β-cell loss (Fig. 6*A*). The rest of NOD mice (mice 1–10) exhibited resting blood glucose levels between 5 and 8 mmol/L (Fig. 6*C*), although their islets were already experiencing varying degrees of immunological assault and β-cell loss (Fig. 6*A*). A profound serum insulin level was observed in one mouse that had fallen in the middle of the disease severity spectrum (Fig. 6*C*, NOD mouse 7). Islets from this specific mouse had severely inflamed islets, and islet destruction had initiated (Fig. 6*A*, mouse 7). DAPI staining showed

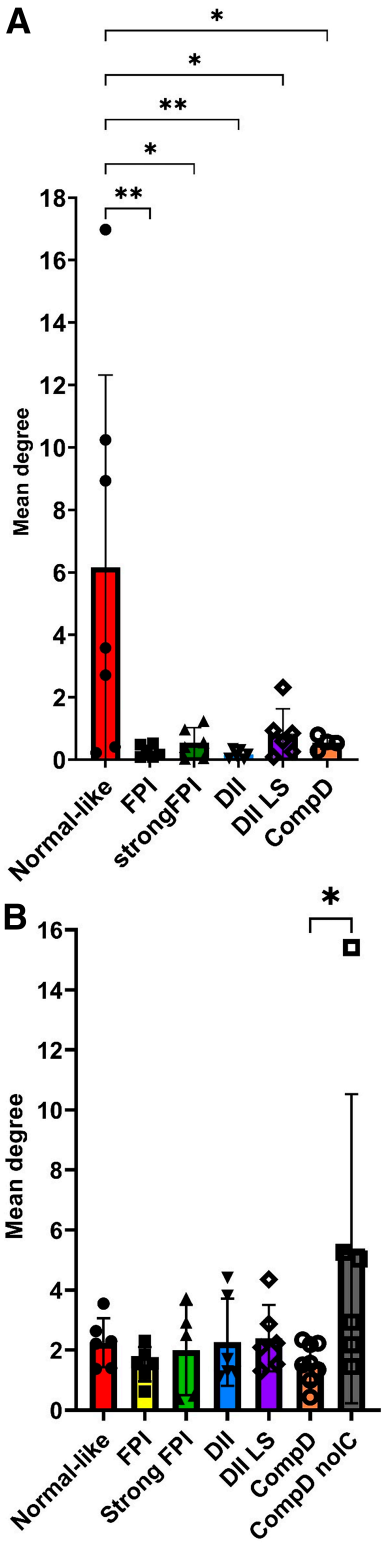


**Figure 5**—Quantification of a network connectivity among β-cells (*A*) and α-cells (*B*) in groups of increasing severity of islet destruction. In *A*, note the mean degree parameter significantly reduced when islet destruction proceeds to FPI group and onward. There is a notable trend of increase in mean degree value in the DII LS group, although statistical significance was not reached. In *B*, note the mean degree value between α-cells significantly increased in the compD no IC stage.

extensive immune cell infiltration in islets within this mouse. The fact that only 1 of the 13 NOD mice exhibited a profoundly high circulating insulin level could suggest that the event of bursting insulin secretion from the islet β-cells happened transiently during the progression the disease.

## DISCUSSION

We demonstrated here for the first time that in the initial phase of islet inflammation in the NOD mice, the β-cells' typical synchronized short $[Ca^{2+}]_c$ events triggered by an 8 mmol/L glucose stimulation disappeared early, whereas the long $[Ca^{2+}]_c$ events emerged more readily at substimulatory 4 and 6 mmol/L glucose conditions. β-cell connectivity was also significantly reduced. During the active islet destruction phase, β-cells revealed some degree of functional recovery, indicated by the transient reappearance of the synchronized short $[Ca^{2+}]_c$ events. However, these events did not persist, likely because of active depletion of islet β-cells. On the other hand, the α-cell $[Ca^{2+}]_c$ events remained glucose sensitive throughout different phases of T1D development. A rather surprising finding was that in the islets with severe β-cell destruction, occasional synchronized $[Ca^{2+}]_c$ events were observed, and α-cell connectivity significantly increased, suggesting potential α-cell networking activities, which may account for the mechanism contributing to glucagon hypersecretion that is clinically observed in T1D patients.

### Potential Mechanisms Underlying the Loss of Short $Ca^{2+}$ Events in β-Cells During T1D Development

In this study, since we aimed at testing fresh islets in pancreas slices, imaging up to six islets per NOD mouse was maximally feasible in each experiment day. These islets have been selected randomly from each NOD mouse in order to best represent the overall islets condition in each mouse.

We observed overt hyperglycemia only in the NOD mice bearing islets that underwent severe immunological assaults and β-cell destruction. Below, we offer possible explanations as to why most NOD mice stayed normoglycemic despite their islets experienced varying degrees of immunogenic assault and β-cell loss.

#### *Altered Pattern of $[Ca^{2+}]_c$ Dynamics in β-Cells During the Development of T1D*

In the initial inflammatory phase, despite the loss of short $[Ca^{2+}]_c$ events, β-cells progressively become more responsive to substimulatory glucose concentrations, as the long $[Ca^{2+}]_c$ events were readily triggered at 4 and 6 mmol/L glucose conditions. We speculate this was a compensatory mechanism of β-cells in order to achieve unaltered circulating insulin levels.

#### *Dysregulated α-Cells During the Development of T1D*

We did not have strong evidence to support this hypothesis, because of larger data variation within the smaller α-cell population in mouse islets, which limited the detection of

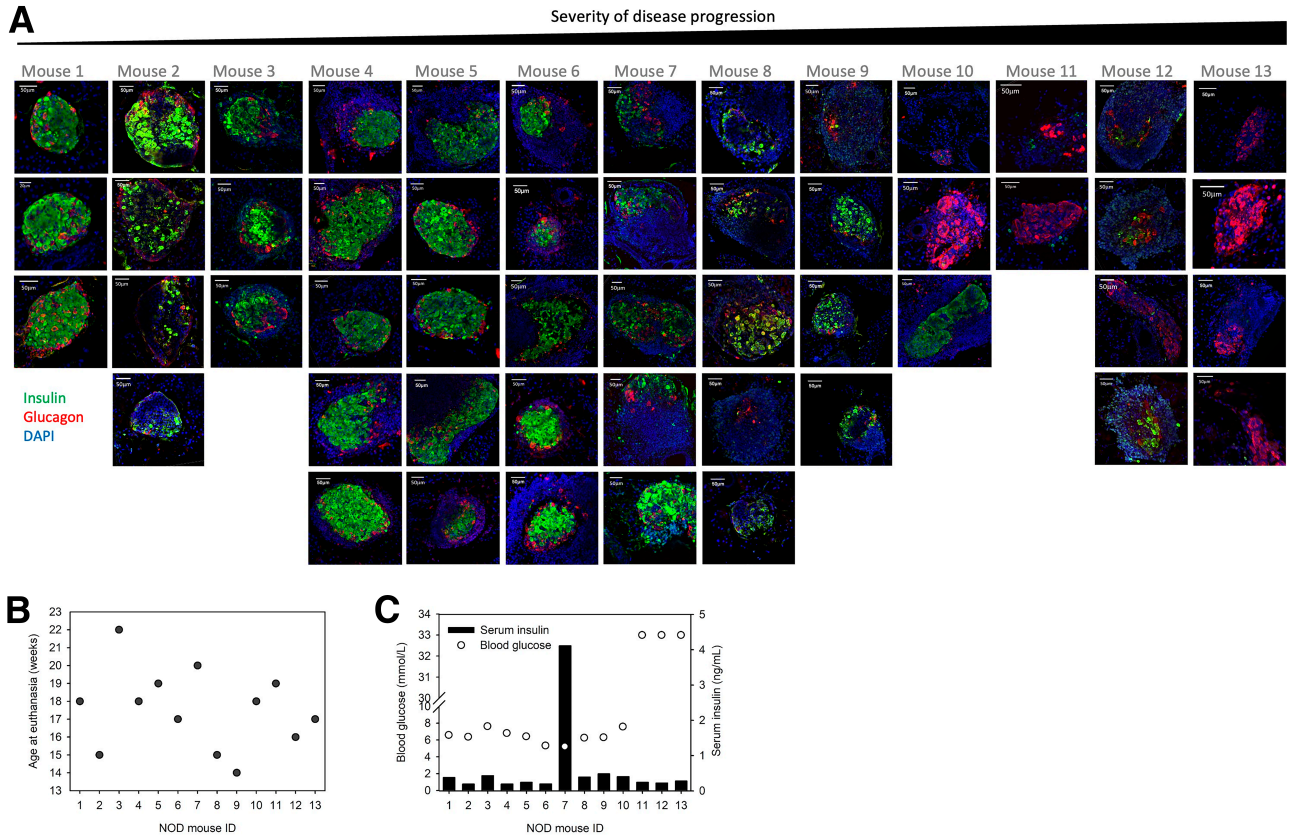


**Figure 6**—Distribution of NOD mice along spontaneous diabetes disease progression. (*A*) Each column represents islets collected from one NOD mouse. Based on the mean islet morphology, severity of β-cell destruction, and immune cell infiltration, a spectrum of NOD mice distributed in the order of spontaneous diabetes disease severity was created. Note that additional islets, which did not undergo $Ca^{2+}$ imaging experiments, were included in this spectrum to help more precisely determine the disease severity of each mouse. (*B*) The NOD mice distribution determined in *A* is plotted as a function of the age of NOD mouse at euthanasia, or (*C*) as a function of blood glucose (circles) and serum insulin (black bars) levels.

milder changes, if any. We also failed to provide serum glucagon measurements in each NOD mouse, because of a shortage of serum collected. Considering that α- and β-cells in the islets tightly regulate each other's function (18), we did observe progressive changes of pattern of both long and short $[Ca^{2+}]_c$ events in β-cells described above. We also observed one NOD mouse in the middle of the T1D severity spectrum exhibiting an overwhelming level of circulating insulin. Both evidences implied the likelihood of altered $[Ca^{2+}]_c$ events in α-cells and the ensuing glucagon secretion. We do recognize that because of the relatively small cohort of NOD mice used in this study, we could not rule out the possibility that the high level of serum insulin found in only 1 of the 13 NOD mice was a technical error, despite the experiments being conducted attentively by highly skilled personnel.

### *Altered δ-Cells Regulations on β-Cell Activity*

A recent report suggested that altering the δ-cell regulation in a healthy islet would subsequently lead to β-cells responding to substimulatory glucose concentration (19). We observed a similar shift of glucose sensitivity in the β-cells in the NOD mice, giving rise to the possibility that the β-cell $[Ca^{2+}]_c$ changes were driven by changes in δ-cell function. However, how the inflammatory milieu surrounding the islet causes the potential δ-cell abnormality in the NOD mice to prime β-cells to be more glucose sensitive warrants further investigations.

### *Intrinsic β-Cell Changes Triggered by the Inflammatory Milieu Surrounding the NOD Mice Islets*

The β-cell $[Ca^{2+}]_c$ temporal profile is shaped collectively by the $Ca^{2+}$ efflux from internal endoplastic reticulum (ER) store and influx from membrane voltage-gated $Ca^{2+}$ channels. It is known that autoimmune assault on T1D islets triggers strong ER stress in β-cells (20). Recently, we further showed that the ER $Ca^{2+}$ release depends on the activity of both ryanodine and $IP_3$ receptors, which could be rendered dysfunctional in autoimmune-stressed conditions, that is, islets in T1D subjects, to cause an ER $Ca^{2+}$ leak (21). It is therefore plausible that the immune cells–and cytokines-induced ER stresses in the β-cells during development of T1D could have caused an improper ER $Ca^{2+}$ leak, explaining why NOD mice islet β-cells have distorted $[Ca^{2+}]_c$ dynamics. Alternatively, the glucose transporters, Glut2, have been found to be downregulated in

the β-cells in T1D mice because of immune cells attack (4), and serum of T1D animals caused increased $[Ca^{2+}]_c$ in healthy mouse β-cells, owing to increased CaV1.2 and CaV1.3 channel density and conductivity (22). Both could be potential mechanisms indirectly or directly altering the $[Ca^{2+}]_c$ dynamics in β-cells of NOD mice.

Finally, the β-cells exhibited a transient recovery of synchronized short $Ca^{2+}$ events during the islet autoimmune destructive phase. It is intriguing how β-cell functions recover. As multiple studies have demonstrated that under conditions of total β-cell ablations in islets of wild-type rodents, active β-cell regeneration occurred early after injury (23–25), we suspected that functional recovery of β-cells was a result of β-cell mass expansion to compensate the loss of β-cells. Indeed, increased β-cell proliferation has been observed in the NOD mouse before diabetes onset (26), likely triggered by the onset of autoimmunity (27).

### Potential Mechanisms Accounting for the Synchronized $[Ca^{2+}]_c$ Events in α-Cells During the Late Phase of Islet Autoimmune Destruction in NOD Mice

We demonstrated synchronized $[Ca^{2+}]_c$ activities among α-cells in the islets found at the later stages of disease progression. Since gap junction expression in rodent α-cells is still debated (28,29), it is unclear how the $[Ca^{2+}]_c$ events in α-cells in the severely disrupted islets in NOD mice become synchronized. Moreover, the pathophysiological implication of these synchronized $[Ca^{2+}]_c$ activities is also unclear. We summarize a few possible explanations:

1. It is known that islets in T1D mouse models remodel actively during T1D development (4,30). This remodeling process could enable α-cells to aggregate and δ-cells to be in closer contact with α-cells, thereby promoting intercellular communications between α-cells and encouraging more efficient or direct regulation of α-cells by δ-cells. Although we have not investigated these possibilities, nor did we provide evidence supporting gap junction expression in α-cells, some, likely paracrine interactions-based, synchronized $Ca^{2+}$ activity in α-cells was observed in islets isolated from healthy mouse (18).
2. It is well-established that intercellular coupling is a classical feature of human and mouse β-cells (31,32). A provocative hypothesis to explain the synchronized activities among the α-cells in the disrupted islets would be that these cells were former β-cells. Transdifferentiation into glucagon-expressing cells allowed them to escape and remain beyond the autoimmune attack during T1D development. This hypothesis is seconded by multiple published works (33–35).
3. Lastly, we concluded that the α-cell synchronized $[Ca^{2+}]_c$ events were unlikely to be neuronal driven. This is based on the facts that during the progression of T1D, both the NOD mice islets and human islets had been characterized by early, sustained, and islet selective loss of sympathetic nerves (36) and that the pancreas slices were acutely disconnected from the central (neural) regulations.

### Limitation of the Study

To date, the technologies currently available do not permit a longitudinal follow-up of islets function over the natural course of T1D development. As such, we randomly sampled "snapshots" of functional characteristics of islets across an age window wherein the female NOD mice are known for progressive diabetes development. A post hoc reconstruction of the sequence of progressive islet destruction in parallel with the functional characteristics we revealed in islets mimicked a "longitudinal" study of the changes of islet α- and β-cell functions along the evolution of islet destruction.

We have included herein a random sample of 45 islets from 13 NOD mice. From our experience, the islets of each NOD mouse, as confirmed in the current study (Supplementary Fig. 2), contribute to two or three out of the seven pathological stages of islets destruction during T1D development. Therefore, the random sampling of two to six islets from a total of 10–15 mice would provide enough islets for each stage to be represented at least five times. With this experimental setting, islets with the least (normal-like) to the most (compD no IC) immunogenic disturbances, namely, from onset to full-blown β-cell destruction, had been identified, confirming that our chosen size of islets and animals was able to cover the entire spectrum of the disease progression. Nonetheless, our experimental setting did not permit us to exclude the possibilities that the islets harboring functionally recovered β-cells were a distinct group of islets that had different starting islet characteristics, or had resisted the immunological attack, or had undergone a pathological islet destruction paradigm different from the destruction sequence defined by islet morphological parameters. To better appreciate our findings, future larger-scale characterization of a greater number of islets from a bigger mouse cohort will help to decipher in finer detail the changes of α- and β-cell function and to encompass the divergent pathological pathways of islet destruction within a T1D diseased pancreas.

Our study tracking the α- and β-cell $[Ca^{2+}]_c$ dynamics during the natural progression of spontaneous diabetes in the NOD mice has provided a detailed overview of the temporal progression of α- and β-cell dysfunctions. We uncovered windows of potential β-cell functional recovery and α-cell synchronization in the islets in NOD mice during T1D development, which would be instrumental for future development of interventional therapies targeting rescue, regeneration, or replenishment of β-cells and amending dysregulated α-cells, allowing T1D patients to better control glycemia.

**Acknowledgments.** M.S.R. received grants from the Austrian Science Fund/Fonds zur Förderung der Wissenschaftlichen Forschung (bilateral grants I3562-B27 and I4319-B30). M.S.R. is a principal investigator on a National Institutes of Health grant (R01DK127236). D.K. and M.S.R. received financial support from the Slovenian Research Agency, Javna Agencija za Raziskovalno Dejavnost RS (research core funding program P3-0396).

**Duality of Interest.** No potential conflicts of interest relevant to this article were reported.

**Author Contributions.** S.P., J.P., S.S., M.S.R., and Y.-C.H. researched and analyzed data. S.S. and D.K. developed the analytical software. Y.-C.H. conceptualized and wrote the manuscript. M.S.R. supervised, edited, and reviewed the manuscript. B.E. and T.P. contributed to manuscript discussion. M.S.R. and Y.-C.H. are the guarantors of this work and, as such, had full access to all the data in the study and take responsibility for the integrity of the data and the accuracy of the data analysis.

## References

1. Gilon P. The role of α-cells in islet function and glucose homeostasis in health and type 2 diabetes. J Mol Biol 2020;432:1367–1394
2. Greenbaum CJ, Prigeon RL, D'Alessio DA. Impaired beta-cell function, incretin effect, and glucagon suppression in patients with type 1 diabetes who have normal fasting glucose. Diabetes 2002;51:951–957
3. Huang YC, Gaisano HY, Leung YM. Electrophysiological identification of mouse islet α-cells: from isolated single α-cells to in situ assessment within pancreas slices. Islets 2011;3:139–143
4. Reddy S, Pathipati P, Bai Y, Robinson E, Ross JM. Histopathological changes in insulin, glucagon and somatostatin cells in the islets of NOD mice during cyclophosphamide-accelerated diabetes: a combined immunohistochemical and histochemical study. J Mol Histol 2005;36:289–300
5. Signore A, Procaccini E, Toscano AM, et al. Histological study of pancreatic beta-cell loss in relation to the insulitis process in the non-obese diabetic mouse. Histochemistry 1994;101:263–269
6. Huang YC, Rupnik M, Gaisano HY. Unperturbed islet α-cell function examined in mouse pancreas tissue slices. J Physiol 2011;589:395–408
7. Huang YC, Rupnik MS, Karimian N, et al. In situ electrophysiological examination of pancreatic α cells in the streptozotocin-induced diabetes model, revealing the cellular basis of glucagon hypersecretion. Diabetes 2013;62:519–530
8. Stožer A, Dolenšek J, Križančić Bombek L, Pohorec V, Slak Rupnik M, Klemen MS. Confocal laser scanning microscopy of calcium dynamics in acute mouse pancreatic tissue slices. J Vis Exp 2021;170:e62293
9. Marciniak A, Cohrs CM, Tsata V, et al. Using pancreas tissue slices for in situ studies of islet of Langerhans and acinar cell biology. Nat Protoc 2014;9:2809–2822
10. Stožer A, Dolenšek J, Rupnik MS. Glucose-stimulated calcium dynamics in islets of Langerhans in acute mouse pancreas tissue slices. PLoS One 2013;8:e54638
11. Stožer A, Gosak M, Dolenšek J, et al. Functional connectivity in islets of Langerhans from mouse pancreas tissue slices. PLOS Comput Biol 2013;9:e1002923
12. Makino S, Kunimoto K, Muraoka Y, Mizushima Y, Katagiri K, Tochino Y. Breeding of a non-obese, diabetic strain of mice. Jikken Dobutsu 1980;29:1–13
13. Speier S, Rupnik M. A novel approach to in situ characterization of pancreatic beta-cells. Pflugers Arch 2003;446:553–558
14. Postić S, Gosak M, Tsai WH, et al. pH-dependence of glucose-dependent activity of beta cell networks in acute mouse pancreatic tissue slice. Front Endocrinol (Lausanne) 2022;13:916688
15. Sluga N, Postić S, Sarikas S, Huang YC, Stožer A, Slak Rupnik M. Dual mode of action of acetylcholine on cytosolic calcium oscillations in pancreatic beta and acinar cells in situ. Cells 2021;10:1580
16. Postić S, Sarikas S, Pfabe J, et al. High-resolution analysis of the cytosolic $Ca^{2+}$ events in β cell collectives in situ. Am J Physiol Endocrinol Metab 2023;324:E42–E55
17. Strandell E, Eizirik DL, Sandler S. Reversal of beta-cell suppression in vitro in pancreatic islets isolated from nonobese diabetic mice during the phase preceding insulin-dependent diabetes mellitus. J Clin Invest 1990;85:1944–1950
18. Ren H, Li Y, Han C, et al. Pancreatic α and β cells are globally phase-locked. Nat Commun 2022;13:3721
19. Ren H, Lee S, Pourhosseinzadeh MS, et al. Paracrine signaling by pancreatic δ cells determines the glycemic set point in mice. 2 July 2022 [preprint]. bioRxiv:2022.06.29.496132
20. Eizirik DL, Colli ML, Ortis F. The role of inflammation in insulitis and beta-cell loss in type 1 diabetes. Nat Rev Endocrinol 2009;5:219–226
21. Yamamoto WR, Bone RN, Sohn P, et al. Endoplasmic reticulum stress alters ryanodine receptor function in the murine pancreatic β cell. J Biol Chem 2019;294:168–181
22. Yang G, Shi Y, Yu J, et al. CaV1.2 and CaV1.3 channel hyperactivation in mouse islet β cells exposed to type 1 diabetic serum. Cell Mol Life Sci 2015;72:1197–1207
23. Bonner-Weir S, Trent DF, Honey RN, Weir GC. Responses of neonatal rat islets to streptozotocin: limited B-cell regeneration and hyperglycemia. Diabetes 1981;30:64–69
24. Thyssen S, Arany E, Hill DJ. Ontogeny of regeneration of beta-cells in the neonatal rat after treatment with streptozotocin. Endocrinology 2006;147:2346–2356
25. Wang RN, Bouwens L, Klöppel G. Beta-cell growth in adolescent and adult rats treated with streptozotocin during the neonatal period. Diabetologia 1996;39:548–557
26. Sreenan S, Pick AJ, Levisetti M, Baldwin AC, Pugh W, Polonsky KS. Increased beta-cell proliferation and reduced mass before diabetes onset in the nonobese diabetic mouse. Diabetes 1999;48:989–996
27. Sherry NA, Kushner JA, Glandt M, Kitamura T, Brillantes AM, Herold KC. Effects of autoimmunity and immune therapy on beta-cell turnover in type 1 diabetes. Diabetes 2006;55:3238–3245
28. Ito A, Ichiyanagi N, Ikeda Y, et al. Adhesion molecule CADM1 contributes to gap junctional communication among pancreatic islet α-cells and prevents their excessive secretion of glucagon. Islets 2012;4:49–55
29. Qiu WL, Zhang YW, Feng Y, Li LC, Yang L, Xu CR. Deciphering pancreatic islet β cell and α cell maturation pathways and characteristic features at the single-cell level. Cell Metab 2017;25:1194–1205.e4
30. Plesner A, Ten Holder JT, Verchere CB. Islet remodeling in female mice with spontaneous autoimmune and streptozotocin-induced diabetes. PLoS One 2014;9:e102843
31. Rutter GA, Hodson DJ, Chabosseau P, Haythorne E, Pullen TJ, Leclerc I. Local and regional control of calcium dynamics in the pancreatic islet. Diabetes Obes Metab 2017;19(Suppl. 1):30–41
32. Skelin Klemen M, Dolenšek J, Slak Rupnik M, Stožer A. The triggering pathway to insulin secretion: functional similarities and differences between the human and the mouse β cells and their translational relevance. Islets 2017;9:109–139
33. Fujita Y, Kozawa J, Fukui K, Iwahashi H, Eguchi H, Shimomura I. Increased NKX6.1 expression and decreased ARX expression in alpha cells accompany reduced beta-cell volume in human subjects. Sci Rep 2021;11:17796
34. Wang YJ, Traum D, Schug J, et al.; HPAP Consortium. Multiplexed in situ imaging mass cytometry analysis of the human endocrine pancreas and immune system in type 1 diabetes. Cell Metab 2019;29:769–783.e4
35. Tang X, Uhl S, Zhang T, et al., SARS-CoV-2 infection induces beta cell transdifferentiation. Cell Metab 2021;33:1577–1591
36. Taborsky GJ Jr., Mei Q, Hackney DJ, Figlewicz DP, LeBoeuf R, Mundinger TO. Loss of islet sympathetic nerves and impairment of glucagon secretion in the NOD mouse: relationship to invasive insulitis. Diabetologia 2009;52:2602–2611